

Article

Study on the Law of Harmful Gas Release from *Limnoperna fortunei* (Dunker 1857) during Maintenance Period of Water Tunnel Based on K-Means Outlier Treatment

Ruonan Wang ¹, Xiaoling Wang ^{2,*}, Songmin Li ^{3,*}, Jupeng Shen ⁴, Jianping Wang ⁵, Changxin Liu ², Yazhi Zheng ², Yitian Chen ¹ and Chaoyuan Ding ²

¹ School of Environmental Science and Engineering, Tianjin University, Tianjin 300350, China; stuwrm@126.com (R.W.); cyttju@163.com (Y.C.)

² State Key Laboratory of Hydraulic Engineering Simulation and Safety, Tianjin University, Tianjin 300072, China; changxin_liu@tju.edu.cn (C.L.); zheng_yazhi@tju.edu.cn (Y.Z.); 2019205110@tju.edu.cn (C.D.)

³ School of Water Conservancy Engineering, Tianjin Agricultural University, Tianjin 300384, China

⁴ Guangdong Yue Hai Pearl River Delta Water Supply Co., Ltd., Guangzhou 511458, China; shenjupeng@gdmail.com

⁵ Guangdong Hydropower Planning & Design Institute, Guangzhou 510635, China; wang.jp@gpdiwe.com

* Correspondence: wangxl@tju.edu.cn (X.W.); lisongmin228@126.com (S.L.)



Citation: Wang, R.; Wang, X.; Li, S.; Shen, J.; Wang, J.; Liu, C.; Zheng, Y.; Chen, Y.; Ding, C. Study on the Law of Harmful Gas Release from *Limnoperna fortunei* (Dunker 1857) during Maintenance Period of Water Tunnel Based on K-Means Outlier Treatment. *Appl. Sci.* **2021**, *11*, 11995. <https://doi.org/10.3390/app112411995>

Academic Editor: Simone Morais

Received: 3 November 2021

Accepted: 10 December 2021

Published: 16 December 2021

Publisher's Note: MDPI stays neutral with regard to jurisdictional claims in published maps and institutional affiliations.



Copyright: © 2021 by the authors. Licensee MDPI, Basel, Switzerland. This article is an open access article distributed under the terms and conditions of the Creative Commons Attribution (CC BY) license (<https://creativecommons.org/licenses/by/4.0/>).

Abstract: It is of great significance for air pollution control and personnel safety guarantee to master the release characteristics of harmful gases in the process of *Limnoperna fortunei* corruption. In view of the lack of research on the environmental pollution caused by the corruption of *Limnoperna fortunei*, a model experiment was designed to study the three harmful gases of NH₃, H₂S, and CH₄ in the putrid process of *Limnoperna fortunei* by considering the density of *Limnoperna fortunei* and the time of leaving water. The results show that: (1) The recognition and processing of outliers based on wavelet decomposition and K-means algorithm can effectively reduce the standard deviation and coefficient of variation of the data set and improve the accuracy of the data set. (2) The variation of NH₃ and H₂S gas concentrations with the time of water separation satisfies polynomial linear regression (R² > 99%). (3) At a density of 0.5–7.0 × 10⁴ mussels/m², the highest concentration of NH₃ reached 47.9777–307.9454 mg/m³ with the increase in the density of *Limnoperna fortunei* and the extension of the time away from water, far exceeding the occupational exposure limit of NH₃ of 30 mg/m³, potentially threatening human health and safety. The highest detection value of H₂S concentration is 0.1909–5.0946 mg/m³, and the highest detection concentration of CH₄ is 0.02%, both of which can be ignored.

Keywords: *Limnoperna fortunei*; corruption laws; the harmful gas; wavelet decomposition; K-means algorithm; outlier identification

1. Introduction

Limnoperna fortunei (dunker 1857) belongs to the Mollusca phylum, bivalve class, and mussel family. The adult mussel is 8–30 mm long, closely connected by byssus, stacked in layers, with a clumpy length of up to 15 cm and a thickness of 3–5 cm [1]. A large number of *Limnoperna fortunei* invade and deposit in pipes, culverts, tunnels, and other structures of water transmission projects, causing structural blockage and corrosion, resulting in serious biological fouling, affecting the normal operation of water transmission projects [2,3]. At present, scholars at home and abroad have carried out a series of studies on its adhesion characteristics, erosion effect on structure, and prevention measures. Through field investigation and statistical analysis, it is found that *Limnoperna fortunei* has strong environmental adaptability in a warm and humid environment, and its reproduction speed and growth amount are amazing [4–6]. Xu et al. [7] investigated the attachment of

Limnoperna fortunei in the pipeline during the maintenance period of water transmission project and obtained the characteristics and rules of *Limnoperna fortunei* invasion into the water transmission pipeline: The attachment density of *Limnoperna fortunei* at the water inlet of the water transfer channel was very high, and the attachment density from the water inlet to the downstream decreased exponentially with the increase in the distance from the water inlet. At the same time, the existence of *Limnoperna fortunei* brings great harm to the project, such as reducing the cross-section area of the pipe, increasing the roughness of the pipe wall, causing wall corrosion, reducing the strength of the concrete structure, and other problems [8–10]. Many scholars have studied the effect of biological fouling control measures on *Limnoperna fortunei* [2,11,12]. It is found that physical control methods such as drying out of water, spraying at high temperature, and regulating water flow, chemical killing methods such as bysalysis and chemical treatment, and biological control methods such as releasing predatory fish can provide guidance for solving biological fouling problems. It can be seen that *Limnoperna fortunei*, as an invasive species in water transportation engineering, has attracted the attention of scholars at home and abroad.

However, the existing researches mainly focus on the impact and prevention of *Limnoperna fortunei* on structural safety, and there is no report on the research on ecological environment safety. During the maintenance period of the water delivery project, a large number of *Limnoperna fortunei* attached to the wall of the cave quickly dehydrated and died in a short period of time, and the rancid smell seriously affected the air quality in the cave and even threatened the safety of maintenance personnel. Some studies showed that fish and shellfish are prone to decay after death. The changes in the initial stage of putrefaction are mainly caused by autolysis, while the later stage of putrefaction is caused by microbial activities [13,14]. A large number of specific putrid bacteria, mainly non-fermented Gram-negative bacteria, grow into the dominant bacteria [15,16], decompose the organism, and produce odor substances such as amine, ammonia, and sulfide [17–19]. According to previous studies, the spoilage bacteria of fish and shrimp products are mainly Enterobacter, H₂S-producing bacteria, and Pseudomonas [20–22]. Under the action of Enterobacter bacteria, amino acids of fish decompose into biological amines and ammonia, sending out a stinky ammonia smell. Under the action of H₂S producing bacteria, sulfur-containing amino acids and cysteine are generated, emitting sulfur odor. Under the action of pseudomonas, shrimp esters produce fruit odor and so on. It can be seen that fish and shellfish and other aquatic organisms are prone to produce putrid substances, which may harm human health when accumulated in large quantities. Therefore, it is very important and urgent to study the release rules of harmful gases in the putrid process of *Limnoperna fortunei*.

At the same time, the release degree of harmful gases during the puffiness of *Limnoperna fortunei* was the result of individual differences and the complexity of microbial reaction. Monitoring data are easily affected by environmental factors, instrument factors, acquisition factors, human factors, etc., and inevitably contain outliers, making concentration data show the characteristics of non-stationary and non-linear changes over time. It is not accurate to use monitoring data directly to analyze and study the complex air pollution in the maintenance period of water tunnel. For abnormal data, the common processing method is to identify discrete points based on statistics, distance, density, or clustering. Dong et al. used the linear interpolation method to replace outliers and the Savitzky-Golay filter method for noise reduction in water quality prediction, and the processed data were integrated into continuous and smooth time series [23]. Aiming at the problem of large errors or outliers in data sets, Sreejith et al. proposed a method that obtains the characteristic distribution model of the data through simulation experiment and then identifies whether the data point is an outlier or not according to the distance between the sampling value and the characteristic model value, for robust regression in the presence of sparse outliers. Finally, the recognition of outlier data is realized, and stable regression is realized in sparse outlier [24]. It is also important to strengthen the identification of monitoring data and the

processing of outliers to analyze the release characteristics of harmful gases from putrefied *Limnoperna fortunei*.

In view of the lack of research on the impact of *Limnoperna fortunei* putrefication on ecological environment safety, three harmful gases, NH_3 , H_2S , and CH_4 , which are highly volatile, irritating, and toxic, were selected as real-time monitoring objects to obtain the change data of gas concentration in the process of *Limnoperna fortunei* putrefication. For the abnormal data, the wavelet decomposition with fast calculation speed, wide application range, and effective retention of signal characteristic points is used to process the complex monitoring data into high and low-frequency basis functions [25,26]. Moreover, the K-means clustering algorithm was used to identify and process the outliers in the high-frequency domain to improve the accuracy of the gas concentration data set. Finally, a mathematical equation was used to quantitatively analyze the discharge law of harmful gases in the putrefication process of *Limnoperna fortunei* to clarify the impact of the putrefication gas pollution on the maintenance environment and personnel. This paper can provide a basis for the subsequent control of harmful gas pollution and guarantee the safety of construction personnel.

2. Tests and Methods

2.1. Collection and Treatment of *Limnoperna fortunei*

In this study, *Limnoperna fortunei* were taken from the wall surface of a warning ship at Taiyuan Pump Station, Qiaotou Town, Dongguan City, Guangdong Province, China ($114^\circ 6' 40.213''$ E, $23^\circ 2' 48.888''$ N, Figure 1). Use a flat-head spade to sample the attached *Limnoperna fortunei*, remove the dead individuals, wash the silt adhered to the byssus and sample surface with clean water and wipe the surface moisture (Figure 2). Use electronic balance to weigh *Limnoperna fortunei* samples. Each sample was measured three times, and the average value of the measured results was recorded as the quality of the sample *Limnoperna fortunei*.

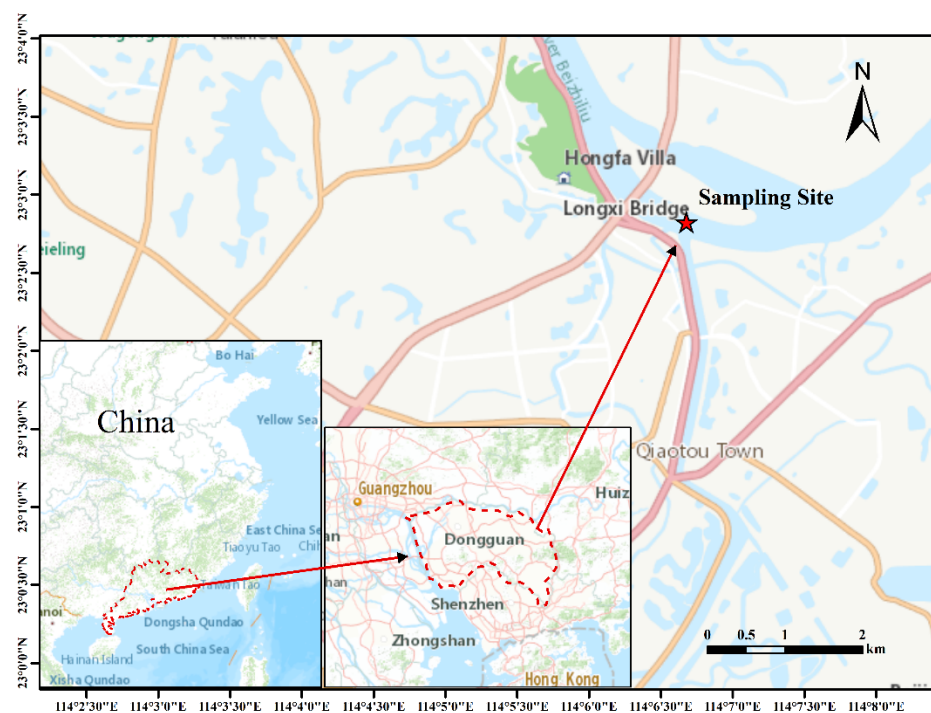


Figure 1. Sampling site of *Limnoperna fortunei*.



Figure 2. *Limnoperna fortunei* sample collection.

2.2. Model Test Design and Operation Monitoring

According to the water pipeline section scale 1:10 design, the test device and the site layout is shown in Figure 3. The device is made of transparent plexiglass, and the gas sampling hole (c) and the reflux hole (d) are set on both sides of the left and right walls. The gas sampling pipe (e) and gas reflux pipe (f) of the online gas detector (g, Model NF-GAS4-200F) are respectively connected, and the multi-purpose hole (b) is used for adding and cleaning *Limnoperna fortunei* (a) before and after the test. The resolutions of NH₃, H₂S, and CH₄ sensors are 0.1 ppm, 0.01 ppm, and 0.1% LEL, respectively. In order to ensure that the temperature, humidity, and other environmental conditions in the device are consistent with the on-site situation, the test is carried out at 30–35 °C. Before the test, the device was filled with water, and then the water was drained to simulate the pipeline maintenance process; finally, the humidity in the device was maintained at 63%~65%RH. In the formal experiment, we put the *Limnoperna fortunei* into the test device and made them die of natural dehydration. The three harmful gases of NH₃, H₂S, and CH₄, as well as environmental factors such as temperature, humidity, and oxygen content during the putrefaction of *Limnoperna fortunei*, were continuously monitored.

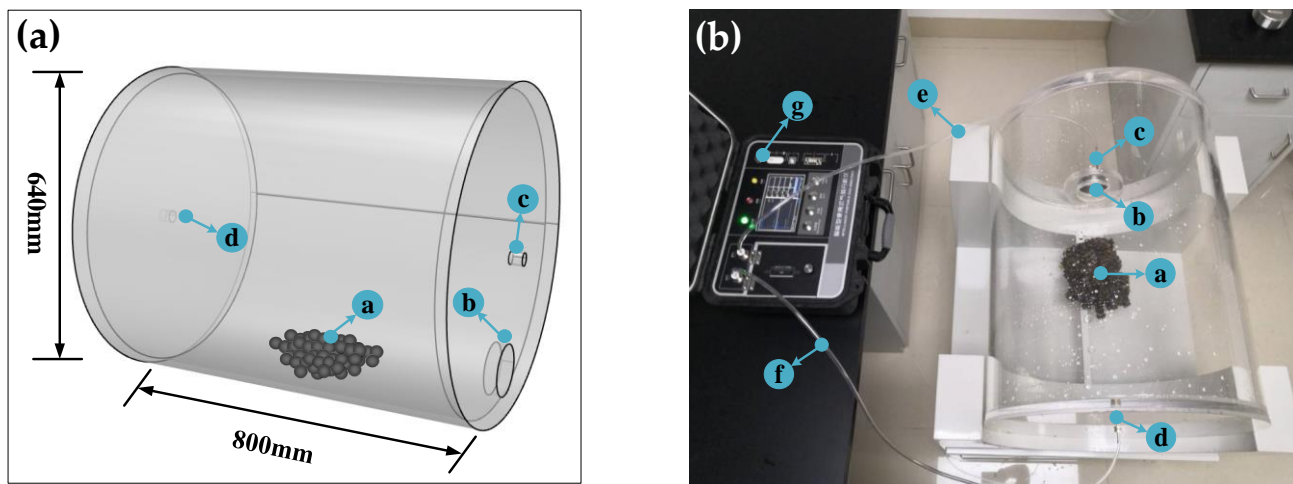


Figure 3. Schematic diagram of test device (a) and site layout (b); (a—mussel cluster; b—multi-purpose hole; c—gas sampling hole; d—gas reflux hole; e—gas sampling pipe; f—gas reflux pipe; g—online gas detector).

According to previous survey results on the distribution law of *Limnoperna fortunei* in the water conveyance tunnel [27], The adhesion density of *Limnoperna fortunei* at the inlet of the water conveyance tunnel is as high as 6.0×10^4 mussels/m², and the density of *Limnoperna fortunei* in the downstream gradually decreases as the distance from the water inlet increases. Considering extreme factors, set up experiments on *Limnoperna fortunei* samples of $0 \sim 7.0 \times 10^4$ mussels/m² and divide the samples with 0.5×10^4 mussels/m² as the gradient interval (Table 1). That is, 50, 100, 150, 200, 250, 300, 350, 400, 450, 500, 550,

600, 650, and 700 *Limnoperna fortunei* were placed on a 0.01 m² plane at the bottom of the device for subsequent tests.

Table 1. Density of *Limnoperna fortunei*.

Number Density ($\times 10^4$ Mussels/m ²)	Samples Size (Mussels/100 cm ²)	Sample Weight (kg/100 cm ²)	Number Density ($\times 10^4$ Mussels/m ²)	Samples Size (Mussels/100 cm ²)	Sample Weight (kg/100 cm ²)
0.5	50	0.0204	4.0	400	0.1465
1.0	100	0.0409	4.5	450	0.1778
1.5	150	0.0645	5.0	500	0.1973
2.0	200	0.0840	5.5	550	0.2133
2.5	250	0.0945	6.0	600	0.2319
3.0	300	0.1146	6.5	650	0.2533
3.5	350	0.1270	7.0	700	0.2803

The test was carried out at Taiyuan Pumping Station, Qiaotou Town, Dongguan City, Guangdong Province, China, from July 2020 to September 2020. The concentration of the three harmful gases NH₃, H₂S, and CH₄ released during the spoilage of the 14 groups of *Limnoperna fortunei* and the changes in the three environmental factors of temperature, humidity, and O₂ in the test device were continuously monitored for a period of 5 days. The data recording frequency of the online gas detector is 1 s/time; that is, the cumulative amount of data for a single indicator in a single set of tests is about 432,000.

2.3. Preprocessing of Gas Concentration Data

In order to maintain stable sensor performance, the equipment will be monitored for 2 min and purged for 20 min after shutdown. The maximum value of all data within 22 min was recorded as the monitoring value of the harmful gas concentration of *Limnoperna fortunei* in this period; that is, about 329 valid data were obtained for each test group. The accuracy of the gas concentration data set can be effectively improved by using wavelet decomposition to extract the high-frequency data and then identifying and processing the outliers combined with a K-means clustering algorithm.

2.3.1. Data Detrending Based on Wavelet Decomposition

The gas concentration data series can be regarded as the superposition of the real signal and the abnormal signal (Equation (1)). That is,

$$C(t) = A(t) + D(t) \quad (1)$$

where $C(t)$ is the original monitoring signal; $A(t)$ is the real signal; $D(t)$ is the abnormal signal.

Wavelet decomposition is a fine purification method for non-stationary time series. According to the characteristics of different wavelet coefficients in the wavelet domain for the effective and abnormal signals in the gas concentration monitoring data, the expansion factor and the translation factor v are changed (Equation (2)), and the signals of different frequencies are decomposed into high-frequency and low-frequency information. Among them, $C(t)$ is the original data information. $A(t)$ array represents the low-frequency data part of each layer, corresponding to the general outline of original data. The $D(t)$ array represents the high-frequency data part of each layer, corresponding to the original data details, and most of the abnormal signals are gathered here. In order to avoid the influence of low-frequency data offset, the analysis is focused on the fluctuation of the data trend itself, and the follow-up calculation is carried out for the high-frequency components.

$$W_f(a, v) = \langle f(t), \psi_{a,v}(t) \rangle = |a|^{-1/2} \int_{\mathbb{R}} f(t) \overline{\psi\left(\frac{t-v}{a}\right)} dt \quad (2)$$

where $a > 0$ is the expansion factor, which mainly adjusts the position and shape of the window. v is the translation factor, which can be positive or negative. It mainly adjusts the

position of the plane time axis window. $f(t)$ is the analysis signal function; $\psi_{a,v}(t)$ is called the fundamental wavelet.

2.3.2. Outlier Recognition Based on K-Means Algorithm

K-means algorithm, also known as the K-means algorithm, is a typical distance-based clustering algorithm, which is widely used in clustering and outlier identification problems due to its clear structure and fast convergence speed [28,29].

The basic idea of the K-means algorithm is that in the gas concentration data set $D = \{X_1, X_2, \dots, X_m\}$, K samples were selected as cluster centers in X_m , namely, the center of mass Z_j ($j = 1, 2, 3, \dots, k$). Calculate the Euclidean distance d_{ij} between each sample X_i ($i = 1, 2, \dots, m$) and K centroids. The samples were divided into clusters with the nearest centroid to obtain K clusters C_j ($j = 1, 2, 3, \dots, k$). The centroid of the new cluster is calculated step by step, and the above steps are repeated until the clustering criterion function converges. The clustering criterion function is shown in Equation (2).

$$\sum_{j=1}^k \sum_{X_i \in C_j} \|X_i - z_j\|_2^2 \quad (3)$$

The E value represents the minimum square error of each cluster after clustering. The smaller the E value is, the closer the gas concentration data in the cluster is around the center of mass. The higher the similarity within the cluster, the better the clustering effect.

2.4. Gas Release Law Analysis

We used the regression analysis method to explore the mathematical relationship between the concentration of harmful gas in *Limnoperna fortunei* and the change of time away from water (Equation (4)). At the same time, the interaction of the concentration of harmful gas released during the putrefying process, the density of *Limnoperna fortunei*, and the time of water release was studied, and the law was quantified (Equation (5)).

$$C = f(t) \quad (4)$$

$$C = f(m, t) \quad (5)$$

where C is the concentration of NH_3 , H_2S , or CH_4 , mg/m^3 ; t is the departure time of *Limnoperna fortunei*, d ; m is the mass density of *Limnoperna fortunei*, mg/m^2 .

In the article, all calculations are performed by the software of matlab 2016 and tablecurve 2D, and all drawings are performed by the software of matlab 2016 and origin 8.0.

3. Results and Discussion

3.1. Morphological Changes of *Limnoperna fortunei* during Putrifaction

The shell of *Limnoperna fortunei* is brown, the abdomen color is lighter, and the double shell is closed. On the first day out of water (Figure 4a), the shells of *Limnoperna fortunei* gradually turned black and brown, and some shells opened and gave off a fishy smell, indicating that the *Limnoperna fortunei* are beginning to die. The next day, the wall of the test device was covered with water mist, and the double shells of the *Limnoperna fortunei* were all opened. The body inside the shell was beige, and it could be seen that the body outline was elliptic. On the third day (Figure 4b), the *Limnoperna fortunei* turned into dark yellow grout, but only a small part of the grout flowed out, and most of the grout was still hanging on the wall inside the *Limnoperna fortunei*. On the fifth day (Figure 4c), the inner body of the shell completely turned into a sticky liquid and scattered around. Only the empty shell existed in the main body of the *Limnoperna fortunei*, and the strong smell of amine filled the box. White mycelium was formed on the surface of the shell after the *Limnoperna fortunei* was placed until the tenth day (Figure 4d).

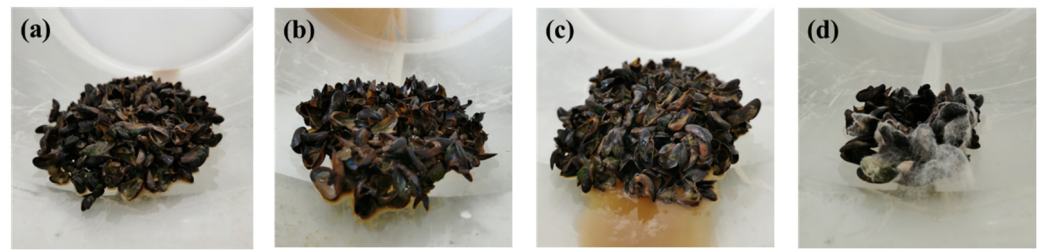


Figure 4. Morphological changes of *Limnoperna fortunei* during putrid process; ((a)—day 1; (b)—day 3; (c)—day 5; (d)—day 10).

3.2. Preprocessing of Gas Monitoring Data

3.2.1. Analysis of the Original Data Set

The ambient temperature in the test device was always maintained at 30–35 °C, the humidity was 63%–65% RH, and the oxygen content was 20.0%–21.0% Vol. The daily variation curve of harmful gas monitoring data in the process of *Limnoperna fortunei* corruption is drawn, as shown in Figures 5 and 6. It can be seen that the release of NH_3 and H_2S has an obvious trend. That is, with the increase in the density of *Limnoperna fortunei* and the extension of time, the accumulation of harmful gas concentration gradually increased. The release concentrations of NH_3 and H_2S in *Limnoperna fortunei* of different densities increased first and then tended to be flat with the extension of time in water, indicating that no NH_3 and H_2S were produced in the middle and late stage of *Limnoperna fortunei* putrefaction. Overall, NH_3 is produced simultaneously with H_2S , but its concentration is significantly lower than H_2S . In all experiments, CH_4 was rarely detected or not detected, and the maximum detected concentration was 0.02%. This concentration is far lower than the exposure limit (1%) defined in *Construction specifications on underground excavation engineering of hydraulic structures* (SL378-2007, 2007) [30], *Code for design of occupational safety and health of water resources and hydropower projects* (GB 50706-2011, 2011) [31] and *Occupational exposure limits for hazardous agents in the workplace-chemical hazardous agents* (GBZ 2.1-2007, 2007) [32], so the subsequent analysis of CH_4 release from the corruption of *Limnoperna fortunei* will not be focused.

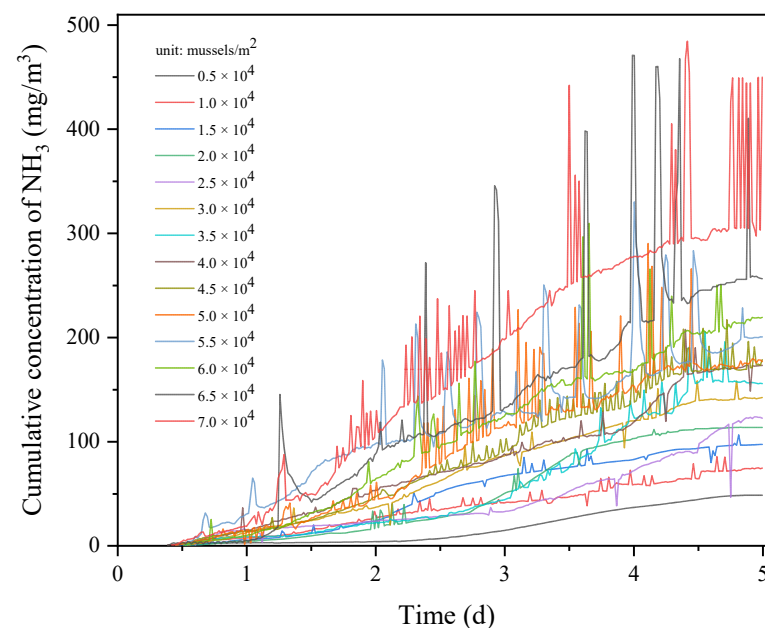


Figure 5. Changes of NH_3 concentration during the putrefaction of *Limnoperna fortunei*.

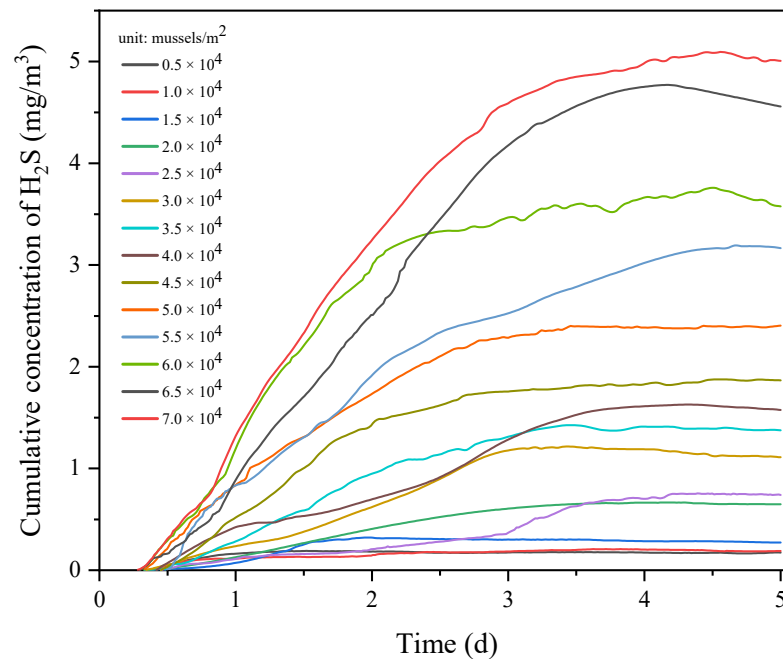


Figure 6. Changes of H₂S concentration during the putrefaction of *Limnoperna fortunei*.

3.2.2. Pretreatment of NH₃ and H₂S Concentration Data

High- and Low-Frequency Signal Features Are Extracted by Wavelet Decomposition

Obviously, NH₃ and H₂S change dynamically with time. It may be caused by the complexity of gas changes and equipment instability. The abnormal signal shows randomness and discontinuity in the time domain. In particular, there are many abnormal points in NH₃, which will seriously affect the accuracy of subsequent analysis if not treated. Each layer of the signal is decomposed into a low-frequency trend part and a high-frequency detail part by using the characteristic that wavelet decomposition can effectively divide non-stationary signal information. Then, the K-means algorithm is used for fine identification and processing of high-frequency outliers to improve the accuracy of the gas concentration data set. This is also the premise and basis of the follow-up study on the harmful gas release in the purification process of *Limnoperna fortunei*.

Db5 wavelet was used to decompose the above data, and the signal diagram as shown in Figure 7 was obtained. After five layers of decomposition, the original concentration data can be divided into a low-frequency array a5 and five high-frequency arrays d1–d5. Compared with a one-dimensional original sequence, arrays in different frequency domains can express potential information of data more effectively and accurately. The amplitude of d1 in the time domain shows randomness, and the main spectrum in the frequency domain is mainly concentrated in the high-frequency domain, containing a large number of outliers. From d1 to d5, the frequency of variation decreases in turn, and the main spectrum is closer to the low-frequency concentration. The frequency of useful signals is mainly concentrated at a5, reflecting the baseline trend of gas concentration.

Identify Outliers of High-Frequency Signals Based on K-Means Algorithm

For gas concentration, the outliers are usually abnormally large or abnormally small. Any outliers will affect the quantitative analysis results of harmful gas release characteristics of *Limnoperna fortunei*, so the outliers in the gas concentration data set were comprehensively identified in this paper. By combining the analysis of the working state of gas monitoring equipment (sensor stability, drift, and failure) and the performance of original sequence data, it is judged that when the number of K-means algorithm clusters is 4, it can not only explain different data conditions but also ensure the stability of clustering results. The identification results of outliers by the K-means algorithm are shown in Figure 8. The

abnormal small values in the concentration of harmful gas are reflected in clusters 1 and 4, and the abnormal large values are reflected in clusters 2 and 3. Among them, cluster no. 1 in the figure is an obviously abnormal small value, and cluster no. 2 is an obviously abnormal large value, which should be directly deleted. Cluster no. 3 and cluster no. 4 are fuzzy outliers, which can be retained or continued processing. By analyzing the overall fluctuation of the sequence, it was empirically determined that cluster 3 and cluster 4 were abnormal data caused by sensor drift, which may affect the accuracy of subsequent quantitative analysis of harmful gas concentration, so it was also deleted.

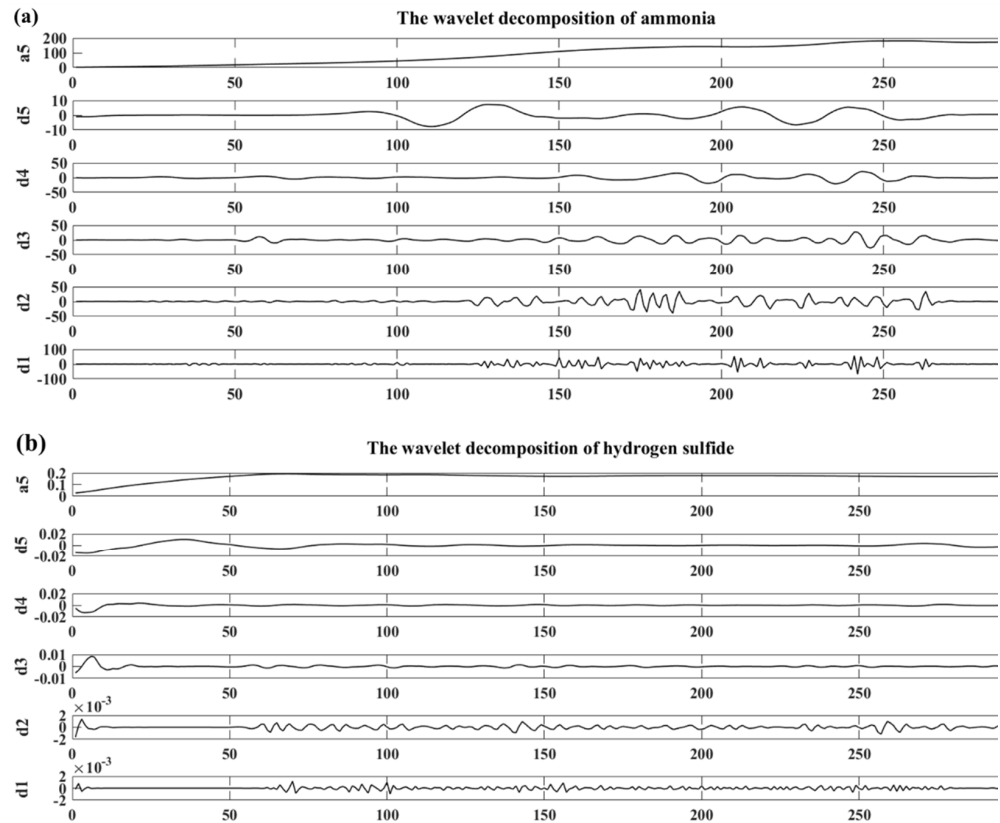


Figure 7. Decomposition of NH₃ (a) and H₂S (b) concentration data by db5 wavelet.

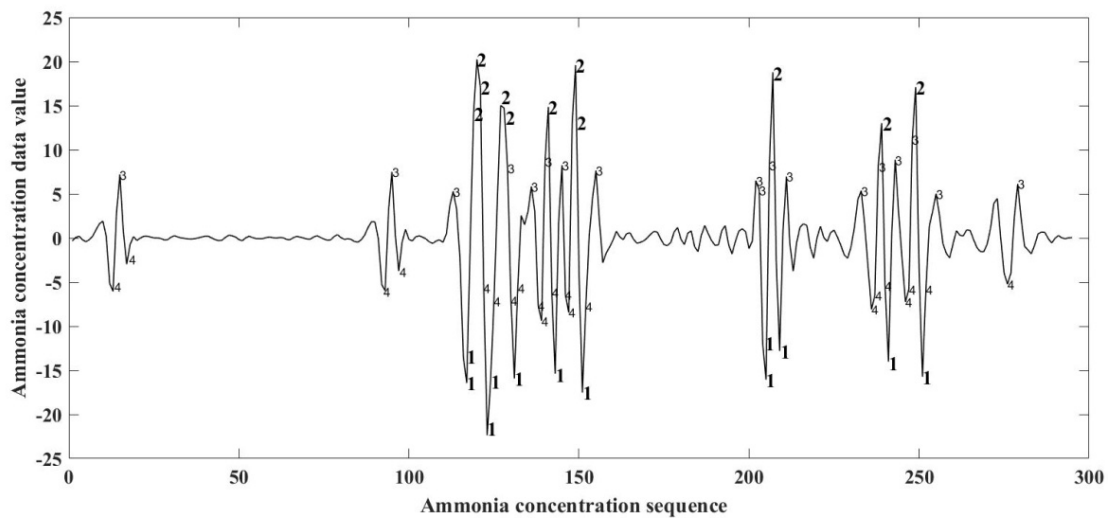


Figure 8. K-means outlier recognition.

The processed high-frequency arrays and the original low-frequency data were reconstructed to obtain a new gas concentration data set, as shown in Figures 9 and 10. Compared with Figures 5 and 6, it can be seen that the change trend of gas concentration is highly consistent with the original monitoring signal, and it is obvious that the graph burr phenomenon decreases and outliers decrease. The evaluation results of the pretreatment effect of gas concentration data are shown in Tables 2 and 3. The standard deviation σ and coefficient of variation CV of each group of data decrease, indicating that the outlier interference is effectively reduced, and the data results processed by the K-means algorithm can be used for subsequent analysis.

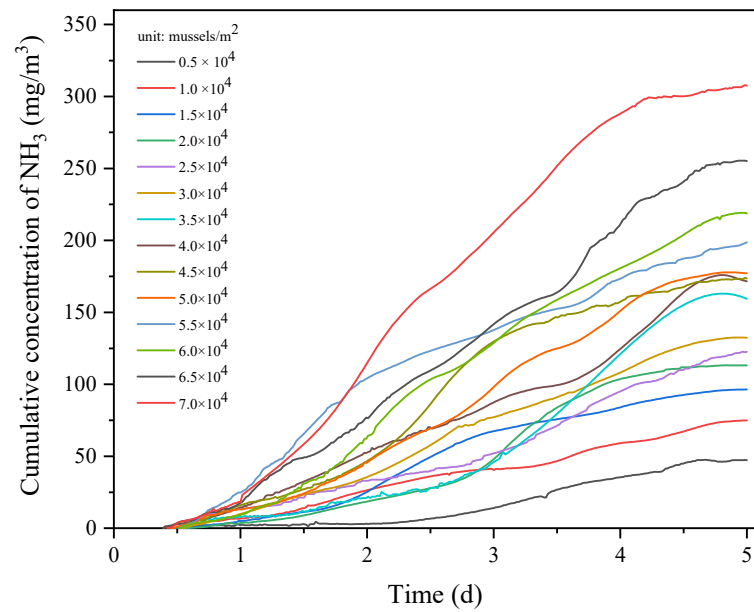


Figure 9. Pretreatment results of NH_3 concentration data.

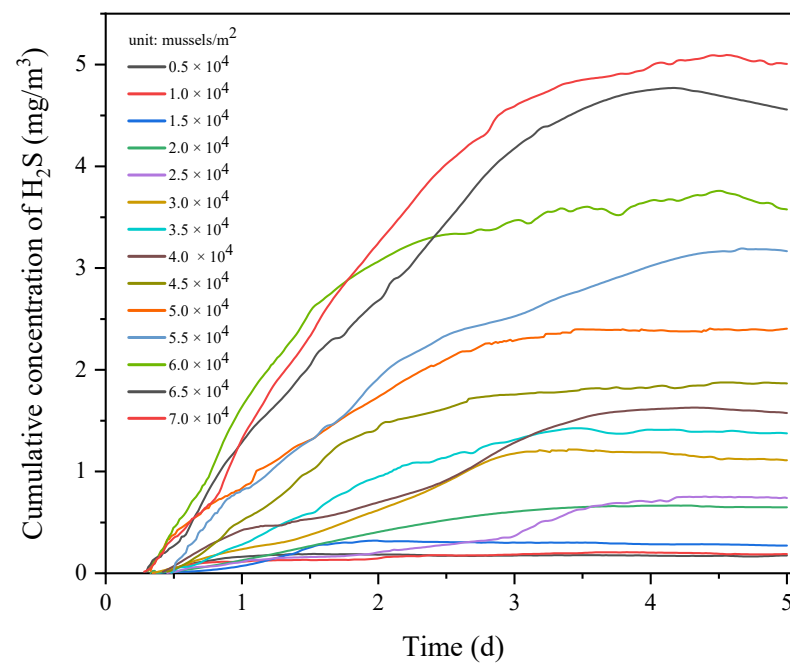


Figure 10. Pretreatment results of H_2S concentration data.

Table 2. Comparison of NH₃ concentration data set before and after repair.

		0.5	1.0	1.5	2.0	2.5	3.0	3.5	4.0	4.5	5.0	5.5	6.0	6.5	7.0
Rawdata	δ	16.767058	22.114135	34.389931	42.714861	33.365958	46.982665	55.987208	52.982421	60.678893	66.830604	64.984631	73.981082	102.485530	118.011266
	\bar{C}	17.770983	37.802422	50.484537	51.662313	44.069167	73.259108	61.901134	79.378196	86.892091	96.132488	122.103267	110.227919	135.060994	175.671261
	CV	0.943508	0.584993	0.681197	0.826809	0.757127	0.641322	0.904462	0.667468	0.698325	0.695193	0.532210	0.671165	0.758809	0.671773
	C_{max}	47.977712	84.960053	105.979206	113.226310	123.215786	157.938219	205.106574	207.160693	216.635426	289.989337	329.960443	309.307054	470.907315	484.512967
Repair data	δ	16.716482	21.991144	34.309874	42.627320	36.779411	42.726538	55.723427	52.958790	61.994448	60.316471	58.361717	72.548227	82.279642	107.003084
	\bar{C}	17.762965	37.784827	50.472732	51.694684	55.346273	66.995734	61.961222	79.515985	95.150493	86.877288	118.946845	110.122408	124.891449	170.771985
	CV	0.941086	0.582010	0.679770	0.824598	0.664533	0.637750	0.899327	0.666014	0.651541	0.694272	0.490654	0.658796	0.658809	0.626585
	C_{max}	47.607156	74.841119	96.445083	113.226300	122.763174	132.529708	162.992975	175.852872	173.959145	177.767343	198.669919	219.128428	255.421770	307.945418

In the table, δ is the standard deviation of NH₃ concentration data; \bar{C} is the average concentration of NH₃; CV is the coefficient of variation of the NH₃ concentration data; C_{max} is the maximum value of the NH₃ concentration data.

Table 3. Comparison of H₂S concentration data set before and after repair.

		0.5	1.0	1.5	2.0	2.5	3.0	3.5	4.0	4.5	5.0	5.5	6.0	6.5	7.0
Rawdata	δ	0.034248	0.044883	0.098694	0.225369	0.259643	0.414985	0.449954	0.519918	0.563922	0.714369	0.909262	1.120077	1.628209	1.636846
	\bar{C}	0.166079	0.160989	0.244019	0.454042	0.399490	0.799765	1.020833	1.032471	1.407727	1.805642	2.169511	2.791567	3.104072	3.509659
	CV	0.206214	0.278797	0.404454	0.496363	0.649936	0.518884	0.440772	0.503566	0.400590	0.395631	0.419109	0.401236	0.524540	0.466383
	C_{max}	0.190918	0.207953	0.322143	0.666502	0.755783	1.217786	1.426353	1.628936	1.875821	2.404795	3.192408	3.758756	4.769833	5.094600
Repair data	δ	0.034246	0.044800	0.098694	0.225068	0.259641	0.414963	0.449953	0.519777	0.563607	0.688696	0.908820	1.018932	1.512646	1.633315
	\bar{C}	0.166080	0.161011	0.244019	0.454195	0.399495	0.799778	1.020833	1.032544	1.407855	1.818383	2.169267	2.887395	3.212002	3.511402
	CV	0.206202	0.278243	0.404451	0.495531	0.649925	0.518847	0.440770	0.503394	0.400331	0.378741	0.418953	0.352890	0.470936	0.465146
	C_{max}	0.190751	0.207947	0.322159	0.666285	0.755245	1.218584	1.426305	1.628952	1.875854	2.406163	3.192408	3.758756	4.769833	5.094600

In the table, δ is the standard deviation of NH₃ concentration data; \bar{C} is the average concentration of NH₃; CV is the coefficient of variation of the NH₃ concentration data; C_{max} is the maximum value of the NH₃ concentration data.

3.3. Release Characteristics of Harmful Gases in the Putrefying Process of *Limnoperna fortunei*
 3.3.1. The Change of Gas Release Concentration with the Time of *Limnoperna fortunei* Leaving Water

According to the monitoring data of gas concentration after pretreatment, the equation of fitting the change of NH₃ and H₂S concentration with the time of leaving water during the putrefying process of *Limnoperna fortunei* is shown in Table 4 (Equations (6)–(19)) and Table 5 (Equations (20)–(33)). The release concentrations of NH₃ and H₂S were linearly correlated with the dewatering time of *Limnoperna fortunei*, satisfying the mathematical model in the form of $C_i = a + bt + ct^{-1} + dt^2 + et^{-2} + ft^3 + gt^{-3} + \dots$ ($R^2 > 99\%$. Where C_i is the release concentration of NH₃ or H₂S, t is how long the mussel is out of water, and $a, b, c, d, e, f, g, \dots$ is the polynomial coefficient). The release concentrations of NH₃ and H₂S in *Limnoperna fortunei* increased first and then tended to be flat with the extension of time in water, indicating that no NH₃ and H₂S were produced in *Limnoperna fortunei* at the end of putrefication. The derivative of the equation can also obtain the change of NH₃ and H₂S release rates over time. The maximum release rates of NH₃ and H₂S were 33.9214–185.5075 mg/(m³·d) and 0.7008–4.0612 mg/(m³·d), respectively, for different attachment densities of *Limnoperna fortunei*.

Table 4. NH₃ release concentration equation of *Limnoperna fortunei* with different densities.

Density ($\times 10^4$ Mussels/m ²)	$C_{NH_3} = f(t)$	R ²	Serial Number
0.5	$C_{NH_3} = -67.40 + 177.43t - 162.42t^2 + 67.29t^3 - 12.10t^4 + 0.78t^5$	99.85%	Equation (6)
1.0	$C_{NH_3} = -197.18 + 674.61t - 850.64t^2 + 514.09t^3 - 155.39t^4 + 22.90t^5 - 1.31t^6$	99.64%	Equation (7)
1.5	$C_{NH_3} = -8567.57 + 3632.71t + 11597.04t^{-1} - 865.62t^2 - 8876.79t^{-2} + 111.16t^3 + 3559.02t^{-3} - 6.00t^4 - 579.90t^{-4}$	99.85%	Equation (8)
2.0	$C_{NH_3} = -129200.02 + 63964.96t + 161762.11t^{-1} - 19662.59t^2 - 121240.38t^{-2} + 3643.32t^3 + 49555.16t^{-3} - 371.30t^4 - 8460.44t^{-4} + 15.94t^5$	99.70%	Equation (9)
2.5	$C_{NH_3} = -21498.92 + 7629.59t + 33605.65t^{-1} - 1413.66t^2 - 29262.01t^{-2} + 122.7735t^3 + 13262.65t^{-3} - 3.48t^4 - 2434.59t^{-4}$	99.78%	Equation (10)
3.0	$C_{NH_3} = 27606.84 - 22319.48t - 17241.65t^{-1} + 10024.78t^2 + 3053.57t^{-2} - 2495.84t^3 + 1734.81t^{-3} + 322.14t^4 - 664.89t^{-4} - 16.81t^5$	99.86%	Equation (11)
3.5	$C_{NH_3} = -13723.15 + 2728.19t + 29123.81t^{-1} + 85.87t^2 - 31631.47t^{-2} - 98.84t^3 + 17259.59t^{-3} + 9.21t^4 - 3750.66t^{-4}$	99.91%	Equation (12)
4.0	$C_{NH_3} = -62439.55 + 23752.51t + 95396.19t^{-1} - 5102.54t^2 - 83605.37t^{-2} + 574.02t^3 + 38844.68t^{-3} - 26.22t^4 - 7395.39t^{-4}$	99.85%	Equation (13)
4.5	$C_{NH_3} = -61187.54 + 21150.84t + 96780.35t^{-1} - 3376.49t^2 - 85768.13t^{-2} + 21.78t^3 + 39910.72t^{-3} + 59.66t^4 - 7583.43t^{-4} - 5.20t^5$	99.86%	Equation (14)
5.0	$C_{NH_3} = -3018.26 + 487.21t + 6684.45t^{-1} + 101.21t^2 - 7447.84t^{-2} - 37.13t^3 + 4128.66t^{-3} + 2.86t^4 - 900.56t^{-4}$	99.80%	Equation (15)
5.5	$C_{NH_3} = -22835.36 + 14906.45t + 20365.84t^{-1} - 5592.57t^2 - 10384.16t^{-2} + 1196.90t^3 + 2795.68t^{-3} - 134.94t^4 - 307.44t^{-4} + 6.19t^5$	99.89%	Equation (16)
6.0	$C_{NH_3} = -657.31 + 562.41t + 304.24t^{-1} - 135.96t^2 - 48.10t^{-2} + 11.06t^3$	99.40%	Equation (17)
6.5	$C_{NH_3} = -3202.07 + 3540.81t + 618.63t^{-1} - 1682.63t^2 + 919.91t^{-2} + 413.65t^3 - 680.61t^{-3} - 50.67t^4 + 180.60t^{-4} + 2.43t^5 - 17.25t^{-5}$	99.70%	Equation (18)
7.0	$C_{NH_3} = -342.53 + 478.91t - 57.15t^{-1} - 119.83t^2 + 110.18t^{-2} + 10.11t^3 - 23.35t^{-3}$	99.80%	Equation (19)

In the table, C_i is the oncentration of H₂S, mg/m³; t is the time out of water, d.

3.3.2. Change of Harmful Gas Concentration with Density of *Limnoperna fortunei*

The change of NH₃ concentration during the purification of *Limnoperna fortunei* is shown in Figure 11. The higher the density of *Limnoperna fortunei*, the higher the maximum release concentration of NH₃. Especially when the number density of *Limnoperna fortunei* reached 5.0–7.0 $\times 10^4$ mussels/m², the maximum NH₃ release concentration increased linearly with the increase in *Limnoperna fortunei* density, from 177.7673 to 307.9454 mg/m³. The fluctuation of the median NH₃ concentration showed no obvious regularity with the change of density of *Limnoperna fortunei*, indicating that the rate of harmful gas release from the putrifaction of *Limnoperna fortunei* was unrelated to the density of *Limnoperna fortunei*, which may be caused by the individual difference of *Limnoperna fortunei* putrifaction and the complexity of microbial reaction.

Table 5. H₂S release concentration equation of *Limnoperna fortunei* with different densities.

Density ($\times 10^4$ Mussels/m ²)	$C_{H_2S} = f(t)$	R ²	Serial Number
0.5	$C_{H_2S} = -17.33 + 7.17t + 24.37t^{-1} - 1.65t^2 - 18.59t^{-2} + 0.20t^3 + 7.07t^{-3} - 0.01t^4 - 1.06t^{-4}$	98.55%	Equation (20)
1.0	$C_{H_2S} = -20.61 + 11.26t + 21.05t^{-1} - 3.31t^2 - 11.33t^{-2} + 0.49t^3 + 2.84t^{-3} - 0.03t^4 - 0.25t^{-4}$	98.20%	Equation (21)
1.5	$C_{H_2S} = -105.84 + 37.75t + 178.28t^{-1} - 7.92t^2 - 172.44t^{-2} + 0.90t^3 + 86.98t^{-3} - 0.04t^4 - 17.62t^{-4}$	98.80%	Equation (22)
2.0	$C_{H_2S} = -64.52 + 36.33t + 69.70t^{-1} - 11.80t^2 - 45.44t^{-2} + 2.16t^3 + 16.37t^{-3} - 0.20t^4 - 2.49t^{-4} + 0.01t^5$	99.95%	Equation (23)
2.5	$C_{H_2S} = -1322.70 + 627.68t + 1726.92t^{-1} - 184.56t^2 - 1351.13t^{-2} + 32.64t^3 + 577.83t^{-3} - 3.18t^4 - 103.55t^{-4} + 0.13t^5$	99.46%	Equation (24)
3.0	$C_{H_2S} = 1816.59 - 679.02t - 3098.72t^{-1} + 161.26t^2 + 3330.02t^{-2} - 23.50t^3 - 2169.67t^{-3} + 1.92t^4 + 779.70t^{-4} - 0.07t^5 - 118.27t^{-5}$	99.75%	Equation (25)
35	$C_{H_2S} = -112.59 + 51.34t + 158.60t^{-1} - 13.59t^2 - 139.81t^{-2} + 1.90t^3 + 68.57t^{-3} - 0.11t^4 - 14.09t^{-4}$	99.76%	Equation (26)
4.0	$C_{H_2S} = -2425.00 + 1240.72t + 2944.31t^{-1} - 393.83t^2 - 2148.75t^{-2} + 75.23t^3 + 860.06t^{-3} - 7.90t^4 - 144.81t^{-4} + 0.35t^5$	99.86%	Equation (27)
4.5	$C_{H_2S} = 99.40 - 47.25t - 109.47t^{-1} + 12.81t^2 + 59.08t^{-2} - 1.82t^3 - 12.44t^{-3} + 0.11t^4$	99.86%	Equation (28)
5.0	$C_{H_2S} = -26.37 + 21.86t + 16.28t^{-1} - 7.87t^2 - 4.86t^{-2} + 1.34t^3 + 0.51t^{-3} - 0.09t^4$	99.84%	Equation (29)
5.5	$C_{H_2S} = -23.43 + 17.18t + 15.44t^{-1} - 4.94t^2 - 4.32t^{-2} + 0.64t^3 + 0.28t^{-3} - 0.03t^4$	99.66%	Equation (30)
6.0	$C_{H_2S} = 69.44 - 34.29t - 66.83t^{-1} + 9.97t^2 + 29.54t^{-2} - 1.52t^3 - 4.89t^{-3} + 0.09t^4$	99.73%	Equation (31)
6.5	$C_{H_2S} = -1042.09 + 575.54t + 1143.17t^{-1} - 189.92t^2 - 736.72t^{-2} + 36.67t^3 + 254.11t^{-3} - 3.82t^4 - 35.95t^{-4} + 0.16t^5$	99.89%	Equation (32)
7.0	$C_{H_2S} = -8.73 + 15.54t - 6.06t^{-1} - 5.66t^2 + 6.79t^{-2} + 0.87t^3 - 1.60t^{-3} - 0.05t^4$	99.95%	Equation (33)

In the table, C_i is the concentration of H₂S, mg/m³; t is the time out of water, d.

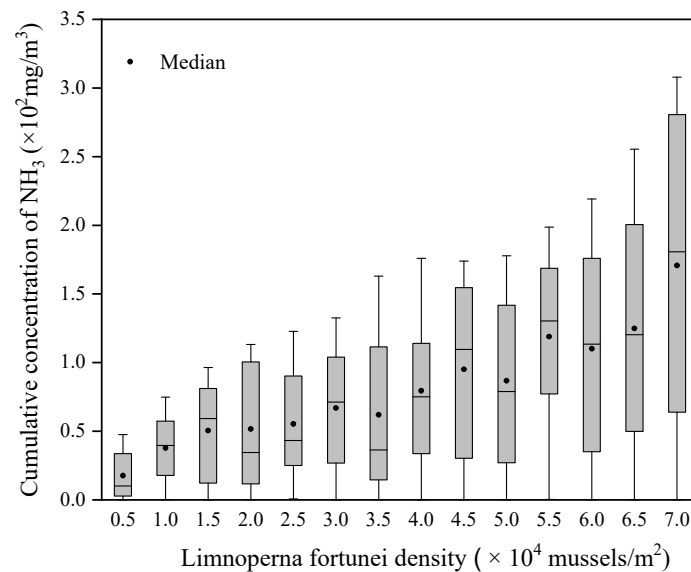


Figure 11. The change of NH₃ concentration under different densities of *Limnoperna fortunei*.

The change of H₂S concentration released by *Limnoperna fortunei* at different densities is shown in Figure 12. The maximum H₂S release concentration was higher when the density of *Limnoperna fortunei* was higher. When the number density of *Limnoperna fortunei* was 0.5–1.5 $\times 10^4$ mussels/m², the release concentration of H₂S was maintained at a low level throughout the whole process of spoilage, and the maximum concentration was not more than 0.3221 mg/m³. When the density of *Limnoperna fortunei* reached 2.5 $\times 10^4$ mussels/m², the release concentration of H₂S increased exponentially, with the density increasing from 0.7552 to 5.0946 mg/m³. In general, the median H₂S concentration increased with the increase in *Limnoperna fortunei* density, which may be related to the early release of H₂S in *Limnoperna fortunei*.

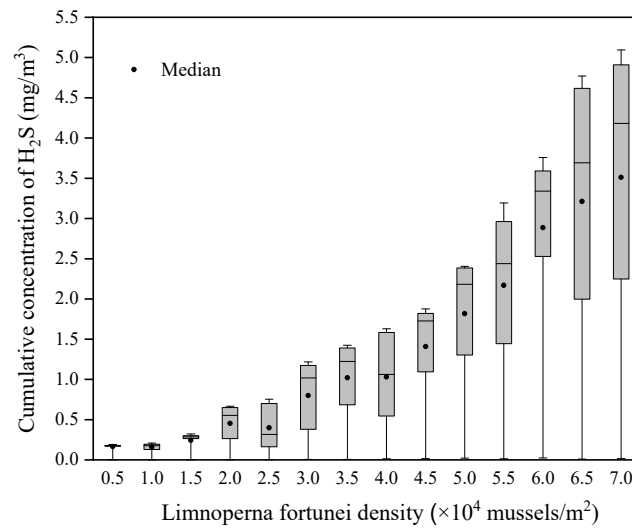


Figure 12. The change of H₂S concentration under different densities of *Limnoperna fortunei*.

3.3.3. Mathematical Model of Harmful Gas Concentration Release Characteristics

In order to further quantify the release law of harmful gases during the putrid process of *Limnoperna fortunei*, the characteristic equation of NH₃ and H₂S concentrations changing with the density of *Limnoperna fortunei* and time out of water was fitted (Equations (34) and (35)). Among them, the gas concentration, the mass density of *Limnoperna fortunei*, and the time out of water are quite different in magnitude. In order to avoid the influence of the above situation on the experimental analysis results, this part of the study has carried out the normalization of the concentration, density, and time data. The complex correlation index R² of NH₃ concentration release characteristic equation is 98.14%, and the root mean square error RMSE value is 0.03143. The complex correlation index R² of the H₂S concentration release characteristic equation is 98.71%, and the root mean square error RMSE is 0.03043. The above model tables all have suitable fitting ability and can be used to estimate the release of NH₃ and H₂S concentration caused by the corruption of *Limnoperna fortunei* based on the distribution rule of *Limnoperna fortunei* and drainage maintenance time in the water pipeline.

$$C_{NH_3} = f(m, t) = \sum_{i=1}^6 \sum_{j=1}^6 a_{ij} m^{i-1} t^{j-1}$$

$$a_{ij} = \begin{bmatrix} -0.0156 & 0.9349 & -7.0490 & 18.8100 & -20.5900 & 7.9130 \\ -0.0315 & -0.6988 & 2.7800 & -5.8740 & 3.2910 & 0 \\ 0.7443 & 3.3820 & 0.6363 & 1.5850 & 0 & 0 \\ -2.2930 & -4.1990 & -2.6180 & 0 & 0 & 0 \\ 3.7020 & 2.6230 & 0 & 0 & 0 & 0 \\ -1.9990 & 0 & 0 & 0 & 0 & 0 \end{bmatrix} \quad (34)$$

where C_{NH₃} is the NH₃ concentration, dimensionless; m is mass density of *Limnoperna fortunei*, dimensionless; t is time out of water, dimensionless.

$$C_{H_2S} = f(m, t) = \sum_{i=1}^6 \sum_{j=1}^6 a_{ij} m^{i-1} t^{j-1}$$

$$a_{ij} = \begin{bmatrix} 0.0200 & -0.8871 & 7.3950 & -22.2400 & 27.2000 & -11.5800 \\ -0.0260 & -1.4920 & 3.5600 & -1.1250 & 0.2000 & 0 \\ 1.2360 & 6.0510 & -3.6330 & 1.6100 & 0 & 0 \\ -4.3470 & -7.3830 & -0.0841 & 0 & 0 & 0 \\ 5.5550 & 3.4290 & 0 & 0 & 0 & 0 \\ -2.4410 & 0 & 0 & 0 & 0 & 0 \end{bmatrix} \quad (35)$$

where C_{H_2S} is the H_2S concentration, dimensionless; m is mass density of *Limnoperna fortunei*, dimensionless; t is time out of water, dimensionless.

3.4. Potential Risk Analysis of Harmful Substances Released by Putrid *Limnoperna fortunei*

The exposure limit of NH_3 is 30 mg/m^3 as defined in *Occupational exposure limits for hazardous agents in the workplace-chemical hazardous agents* (GBZ 2.1-2007, 2007) [32] and other relevant specifications. In this experiment, the concentration of NH_3 in *Limnoperna fortunei* with a density of $6.0\text{--}7.0 \times 10^4$ mussels/ m^2 reached the contact limit on the first day after the *Limnoperna fortunei* was out of water. On the second day out of water, the concentration of NH_3 in *Limnoperna fortunei* with a density of $4.5\text{--}5.5 \times 10^4$ mussels/ m^2 reached the contact limit. On the third day out of water, the concentration of NH_3 reached the contact limit for all *Limnoperna fortunei* with a density of $0.5\text{--}4.0 \times 10^4$ mussels/ m^2 . In particular, NH_3 concentration reached the highest detected value of 307.9454 mg/m^3 when the density of *Limnoperna fortunei* was 7.0×10^4 mussels/ m^2 and the time in water was 4.8 days. It can be seen that the concentration of NH_3 released during the spoilage of *Limnoperna fortunei* can reach the level of health and safety threat to workers in a short period of time, and the cumulative concentration of NH_3 is far beyond the exposure limit with the increase in the time when *Limnoperna fortunei* are away from water. Therefore, the influence of NH_3 pollutants should be considered in the spoilage and pollution control of *Limnoperna fortunei*.

When the density of *Limnoperna fortunei* is 7.0×10^4 mussels/ m^2 and the time of water separation is 3d, the highest value of H_2S concentration detection data is 5.0946 mg/m^3 , which is lower than the H_2S exposure limit of 10 mg/m^3 defined in *Occupational exposure limits for hazardous agents in the workplace-chemical hazardous agents* (GBZ 2.1-2007, 2007) [32] and other relevant specifications. That is, the H_2S concentration produced during the corruption of *Limnoperna fortunei* has an acceptable influence on the staff.

NH_3 causes mucosal diseases of the eye and respiratory system and even causes coma, shock, and respiratory distress syndrome, and inhaling a small amount of high concentration of H_2S can be fatal in a short time. After the overhaul and drainage, the air circulation condition in the water pipeline is poor, so the ventilation environment standard during the overhaul should be formulated in accordance with the relevant specifications in time, and the oxygen content, the scope of the overhaul wind speed, and the maximum allowable content of harmful gases should be clear, in order to avoid the *Limnoperna fortunei* corruption and the release of harmful gases threatening the health and safety of maintenance personnel.

4. Conclusions

In view of the lack of research on the environmental effects of invasive organisms in water transport projects, this paper designed a model test to study the harmful gases NH_3 , H_2S , and CH_4 released during the putrid process of *Limnoperna fortunei* and quantitatively explored the relationship between their concentrations and the time when *Limnoperna fortunei* leaves water and the density of *Limnoperna fortunei* attachment. The main conclusions are as follows:

1. For outliers in the original gas concentration data set, wavelet decomposition and K-means algorithm are used to identify and process outliers, which can effectively reduce the standard deviation and coefficient of variation of the data set and improve the accuracy of the data set;
2. NH_3 is the main harmful gas released in the process of purification, followed by H_2S , with a maximum concentration of 307.9454 mg/m^3 and 5.0946 mg/m^3 , respectively. Only a very small amount of CH_4 was detected during the process, and the maximum concentration did not exceed 0.02%;
3. The quantitative relationship between NH_3 and H_2S and *Limnoperna fortunei* density and dewatering time all met the n-order polynomial linear regression model

- ($R^2 > 99\%$), that is, with the increase in *Limnoperna fortunei* density or dewatering time, the concentration of NH_3 and H_2S gradually increased;
- The concentration of NH_3 released during the corruption of *Limnoperna fortunei* can reach the level of health and safety threat to workers at the earliest day out of water, and the accumulated concentration of NH_3 far exceeds the exposure limit (30 mg/m^3) with the increase in the time out of water of *Limnoperna fortunei*. The influence of H_2S and CH_4 concentration on workers is still within an acceptable level.

Author Contributions: R.W.: Methodology, Investigation, Data curation, Writing—original draft. X.W. and S.L.: Methodology, Supervision, Writing—review and editing. J.S.: Resources, Supervision. J.W.: Resources, Validation. C.L.: Data curation, Visualization. Y.Z.: Investigation, Data curation. Y.C.: Investigation, Writing—review and editing. C.D.: Investigation, Visualization. All authors have read and agreed to the published version of the manuscript.

Funding: This research was funded by [Natural Science Foundation of Tianjin, China] grant number [No. 19JCYBJC22600].

Institutional Review Board Statement: Not applicable.

Informed Consent Statement: Not applicable.

Data Availability Statement: The data that support the findings of this study are available from the corresponding author upon reasonable request.

Acknowledgments: The authors are grateful for the support from the State Key Laboratory of Hydraulic Engineering Simulation and Safety at Tianjin University and the Guangdong Yue Hai Pearl River Delta Water Supply Co., Ltd., China.

Conflicts of Interest: The authors declare that they have no known competing financial interests or personal relationships that could have appeared to influence the work reported in this paper.

References

- Furlan-Murari, P.J.; Ruas, C.D.F.; Ruas, E.A.; Benício, L.M.; Urrea-Rojas, A.M.; Poveda-Parra, A.R.; Murari, E.; De Lima, E.C.S.; De Souza, F.P.; Lopera-Barrero, N.M. Structure and genetic variability of golden mussel (*Limnoperna fortunei*) populations from Brazilian reservoirs. *Ecol. Evol.* **2019**, *9*, 2706–2714. [[CrossRef](#)]
- Boltovskoy, D.; Xu, M.; Nakano, D. *Impacts of Limnoperna Fortunei on Man-Made Structures and Control Strategies: General Overview*; Springer: Singapore, 2015; pp. 375–393.
- Magara, Y.; Matsui, Y.; Goto, Y.; Yuasa, A. Invasion of the non-indigenous nuisance mussel, *Limnoperna fortunei*, into water supply facilities in Japan. *J. Water Supply Res. Technol.* **2001**, *50*, 113–124. [[CrossRef](#)]
- Ernandes-Silva, J.; Pinha, G.D.; Mormul, R.P. Environmental variables driving the larval distribution of *Limnoperna fortunei* in the upper Paraná River floodplain, Brazil. *Acta Limnol. Bras.* **2017**, *29*, 108. [[CrossRef](#)]
- Darrigran, G.; Damborenea, C.; De Drago, I.E.; Paira, A.R.; Drago, E.C.; Archuby, F. Invasion process of *Limnoperna fortunei* (Bivalvia: Mytilidae): The case of Uruguay River and emissaries of the Esteros del Iberá Wetland, Argentina. *Zoologia* **2012**, *29*, 531–539. [[CrossRef](#)]
- Pessotto, M.A.; Nogueira, M.G. More than two decades after the introduction of *Limnoperna fortunei* (Dunker 1857) in La Plata Basin. *Braz. J. Biol.* **2018**, *78*, 773–784. [[CrossRef](#)]
- Xu, M.; Wang, Z.; Zhao, N. Experimental study of colonization of *Limnoperna fortunei* (dunker 1857) in the Xizhijiang River. In Proceedings of the Blueprint for Sustainable Watersheds Workshop Beijing, Beijing, China, 31 July–4 August 2011.
- Darrigran, G. Potential Impact of Filter-feeding Invaders on Temperate Inland Freshwater Environments. *Biol. Invasions* **2002**, *4*, 145–156. [[CrossRef](#)]
- Brugnoli, E.; Clemente, J.; Boccardi, L.; Borthagaray, A.; Scarabino, F. Golden mussel *Limnoperna fortunei* (Bivalvia: Mytilidae) distribution in the main hydrographical basins of Uruguay: Update and predictions. *An. Acad. Bras. Ciências* **2005**, *77*, 235–244. [[CrossRef](#)] [[PubMed](#)]
- De Oliveira, M.D.; Takeda, A.M.; de Barros, L.F.; Barbosa, D.S.; de Resende, E.K. Invasion by *Limnoperna fortunei*(Dunker,1857) (Bivalvia, Mytilidae)of the Pantanal Wetland, Brazil. *Biol. Invasions* **2006**, *18*, 97–104. [[CrossRef](#)]
- Xu, M.; Darrigran, G.; Wang, Z.; Zhao, N.; Lin, C.C.; Pan, B. Experimental study on control of *Limnoperna fortunei* biofouling in water transfer tunnels. *HydroResearch* **2015**, *9*, 248–258. [[CrossRef](#)]
- Zhang, C.; Xu, M.; Wang, Z.; Liu, W.; Yu, D. Experimental study on the effect of turbulence in pipelines on the mortality of *Limnoperna fortunei* veligers. *Ecol. Eng.* **2017**, *109*, 101–118. [[CrossRef](#)]

13. Ocaño-Higuera, V.; Marquez-Ríos, E.; Canizales-Dávila, M.; Castillo-Yáñez, F.; Pacheco-Aguilar, R.; Sanchez, M.E.L.; García-Orozco, K.; Graciano-Verdugo, A.Z. Postmortem changes in cazon fish muscle stored on ice. *Food Chem.* **2009**, *116*, 933–938. [[CrossRef](#)]
14. Peck, M.W.; Stringer, S.C. The safety of pasteurised in-pack chilled meat products with respect to the foodborne botulism hazard. *Meat Sci.* **2005**, *70*, 461–475. [[CrossRef](#)] [[PubMed](#)]
15. Gram, L.; Dalgaard, P. Fish spoilage bacteria—problems and solutions. *Curr. Opin. Biotechnol.* **2002**, *13*, 262–266. [[CrossRef](#)]
16. Dalgaard, P. Modelling of microbial activity and prediction of shelf life for packed fresh fish. *Int. J. Food Microbiol.* **1995**, *26*, 305–317. [[CrossRef](#)]
17. Doyle, M.P. *Food Microbiology: Fundamentals and Frontiers*, 3rd ed.; ASM Press: Washington, DC, USA, 2007.
18. Wang, H.; Zhang, J.; Zhu, Y.; Wang, X.; Shi, W. Volatile components present in different parts of grass carp. *J. Food Biochem.* **2018**, *42*, e12668. [[CrossRef](#)]
19. Wang, H.; Zhu, Y.; Zhang, J.; Wang, X.; Shi, W. Study on changes in the quality of grass carp in the process of postmortem. *J. Food Biochem.* **2018**, *42*, e12683. [[CrossRef](#)]
20. Vogel, B.F.; Venkateswaran, K.; Satomi, M.; Gram, L. Identification of *Shewanella baltica* as the Most Important H₂S-Producing Species during Iced Storage of Danish Marine Fish. *Appl. Environ. Microbiol.* **2005**, *71*, 6689–6697. Available online: <http://jama.jamanetwork.com/article.aspx?articleid=294000> (accessed on 1 November 2021). [[CrossRef](#)] [[PubMed](#)]
21. Dabadé, D.S.; Azokpota, P.; Nout, M.R.; Hounhouigan, D.J.; Zwietering, M.H.; Besten, H.M.D. Prediction of spoilage of tropical shrimp (*Penaeus notialis*) under dynamic temperature regimes. *Int. J. Food Microbiol.* **2015**, *210*, 121–130. [[CrossRef](#)]
22. Wang, H.; Luo, Y.; Huang, H.; Xu, Q. Microbial succession of grass carp (*Ctenopharyngodon idellus*) filets during storage at 4 °C and its contribution to biogenic amines' formation. *Int. J. Food Microbiol.* **2014**, *190*, 66–71. [[CrossRef](#)]
23. Dong, Q.; Lin, Y.; Bi, J.; Yuan, H. An Integrated Deep Neural Network Approach for Large-Scale Water Quality Time Series Prediction. In Proceedings of the 2019 IEEE International Conference on Systems, Man and Cybernetics (SMC), Bari, Italy, 6–9 October 2019.
24. Kallummil, S.; Kalyani, S. Noise Statistics Oblivious GARD For Robust Regression With Sparse Outliers. *IEEE Trans. Signal Process.* **2018**, *67*, 383–398. [[CrossRef](#)]
25. Mallat, S.G.A. Theory for Multiresolution Signal Decomposition: The Wavelet Representation. *IEEE Trans. Pattern Anal. Mach. Intell.* **1989**, *11*, 674–693. [[CrossRef](#)]
26. Mallat, S.; Hwang, W.L. Singularity Detection and Processing with Wavelets. *IEEE Trans. Inf. Theory* **1992**, *38*, 617–643. [[CrossRef](#)]
27. Xu, M.Z.; Wang, Z.Y.; Duan, X.H.; Zhuang, M.Q.; de Souza, F.T. Ecological measures of controlling invasion of golden mussel (*Limnoperna fortunei*) in water transfer systems. In Proceedings of the 33rd IAH Congress, Water Engineering for A Sustainable Environment, Vancouver, BC, Canada, 9–14 August 2009; pp. 1609–1616.
28. Bai, L.; Liang, J.; Sui, C.; Dang, C. Fast global k-means clustering based on local geometrical information. *Inf. Sci.* **2013**, *245*, 168–180. [[CrossRef](#)]
29. Zhang, Z.; Feng, Q.; Huang, J.; Guo, Y.; Xu, J.; Wang, J. A local search algorithm for k-means with outliers. *Neurocomputing* **2021**, *450*, 230–241. [[CrossRef](#)]
30. *Construction Specifications on underground Excavation Engineering of Hydraulic Structures: SL378-2007*; Ministry of Water Resources of the People's Republic of China: Beijing, China, 2007; pp. 53–54. (In Chinese)
31. *Code for Design of Occupational Safety and Health of Water Resources and Hydropower Projects: GB 50706-2011*; National Standards of People's Republic of China: Beijing, China, 2011; p. 15. (In Chinese)
32. *Occupational Exposure Limits for Hazardous Agents in the Workplace-Chemical Hazardous Agents: GBZ 2.1-2007*; National Health Commission of the People's Republic of China: Beijing, China, 2007; pp. 3–16. (In Chinese)